Threshold selection in transform-domain denoising of speckle pattern fringes

Assen A. Shulev*[a], Atanas Gotchev[b], Alessandro Foi[b], Ilia R. Roussev[c]
[a] Central Laboratory of Optical Storage and Processing of Information – BAS, bl. 101 Acad. G. Bonchev St., 1113 Sofia, Bulgaria
[b] Institute of Signal Processing – Tampere University of Technology, FIN-33101 Tampere, Finland
[c] Institute of Mechanics – BAS, bl. 4 Acad. G. Bonchev St., 1113 Sofia, Bulgaria

ABSTRACT

A transform-domain fringe pattern denoising technique is presented. The Discrete Cosine Transform (DCT) is applied in a sliding window manner to get an overcomplete image expansion, and then the transform coefficients are thresholded to reduce the noise. We investigate the proper size of the sliding window and the proper threshold level. The latter is determined individually for each window position using a local noise variance estimate. In order to deal with a rather inadequate but simplified noise model, a proportionality factor, related with the speckle size, is found by experiments with digitally simulated speckle fringes. Such a proportionality factor suggests that the technique could be made fully automatic. We demonstrate promising results in denoising of real speckle fringe patterns, obtained through an out-of-plane sensitive Digital Speckle Pattern Interferometry (DSPI) set-up in a process of non-destructive testing of reinforced composite materials deformation.

Keywords: Speckle noise, local transforms, Fourier transform, discrete cosine transform, digital speckle pattern interferometry

1. INTRODUCTION

Digital Speckle Pattern Interferometry (DSPI) is a well developed experimental method for non-destructive quantitative and qualitative testing. It offers high degree of accuracy in measuring micro and sub-micro displacements of roughly scattering surfaces induced from deformations of the investigated object. Variety of DSPI algorithms and measurement configurations has been proposed [1-3]. However, the intrinsic noisy character of the speckle fringe patterns decreases the measurements accuracy. For such patterns, the signal to noise ratio is close to unity and the contrast across the pattern periphery is poor due to the normally used Gaussian illumination [4].

In order to reduce the noise and to enhance the contrast of correlation fringe patterns various algorithms have been developed. Standard spatial-domain speckle filters, such as median, mean or low-pass filters, Gamma, Frost, and geometric filters usually over-smooth or does not suppress the noise efficiently [5, 6]. Recursive techniques could result in less oversmoothing for the price of excessive bias [7]. Recently, transform-domain denoising techniques have proven superior for a large variety of real images. Several factors are crucial for such techniques, i.e. good localization properties of the transforms chosen, high factor of over-completeness of the transform and proper threshold selection. Localization is preferable as it ensures different treatment of homogeneous image regions and regions with image details [8]. Over-completeness ensures multiple estimates of each pixel thus reducing the border effects arising from the local processing. The threshold is depending essentially on the statistical properties of the noise and therefore should be elaborated carefully for the image class and noise model under study.

In DSPI field several attempts to utilize transform-domain denoising have been made, either wavelet [9, 10] or Fourier-based [11, 12]. The wavelet techniques reported in ref. [10] apply no over-complete transforms and rely on classical threshold [13] or even on sub-band removal that is essentially a simple low-pass filtering. The Fourier technique in ref.

[12] suggests using a visually-adjusted interactive threshold. While it demonstrates preservation of the fine fringe structure, it is clearly non-automatic and lacks quantitative basis.

The aim of this contribution is two-fold. First, it demonstrates the applicability of discrete cosine transform in denoising fringe patterns. Second, it gives account on the suitable choice of the window size and threshold level. As obtaining a precise noise model is rather difficult we aim at finding a proportionality factor, which would adjust the threshold for a simplified model properly. The assessment is done by processing of synthesized speckle patterns where the noise-free patterns are known. Real correlation fringes are also processed in order to demonstrate the possibility of having a fully automated transform-domain denoising technique.

2. SPECKLE PATTERN FRINGES MODEL

We adopt a classical optical arrangement to produce speckle patterns generated by rough scattering surface [10], as illustrated in Fig. 1.

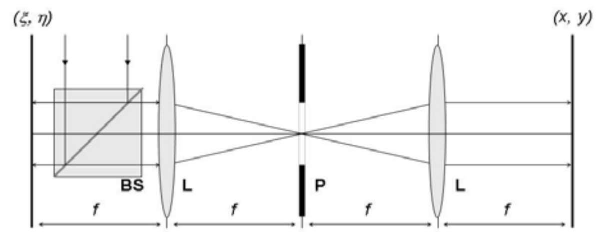

Fig. 1. Optical set-up for speckle pattern generation: BS - beam splitter; L - lenses; P - pupil stop

The rough surface is normally illuminated by a coherent Gaussian beam $G(\xi, \eta)$ via the beam splitter BS. The two lenses L are with equal focal lengths f and the diameter of the pupil stop P in the focal plane is d. The amplitudes of the electric fields reflected from the rough surface before and after a small deformation are:

$$a_i(\xi,\eta) = G(\xi,\eta) r \exp[i\varphi(\xi,\eta)], \quad a_f(\xi,\eta) = G(\xi,\eta) r \exp\left[i(\varphi(\xi,\eta)+\phi(\xi,\eta))\right], \tag{1}$$

where r is the average reflectivity of the scattering surface, $\varphi(\xi, \eta)$ is the random phase uniformly distributed in the interval $[-\pi, \pi]$ and $\phi(\xi, \eta)$ is the phase change which corresponds to the deformation of the surface. The amplitudes before and after the deformation in the observation plane (x, y) can be presented as:

$$A_i(x,y) \approx F^{-1}\{t(u,v)F\{a_i(\xi,\eta)\}\}, \quad A_f(x,y) \approx F^{-1}\{t(u,v)F\{a_f(\xi,\eta)\}\}, \tag{2}$$

where F and F^{-1} denotes the right and inverse Fourier transforms respectively, $t(u, v) = \mathrm{circ}(\rho)$ is circular low-pass filter in the frequency domain with radius ρ which corresponds to the pupil stop P in the experimental set-up [10, 14]. If we assume an interferometer with out-of-plane sensitivity and amplitude of the reference beam $A_r(x, y)$ then the interference patterns in the observation plane are:

$$I_i(x,y) = \left|A_i(x,y) + A_r(x,y)\right|^2, \quad I_f(x,y) = \left|A_f(x,y) + A_r(x,y)\right|^2. \tag{3}$$

The DSPI fringes can be presented as the absolute value of the difference between two speckle intensity fields:

$$I(x,y) = \left|I_f(x,y) - I_i(x,y)\right|. \tag{4}$$

To simulate the decorrelation effect, an independent speckle beam can be added to the initial non-deformed state of the object [15]:

$$a_i(\xi,\eta) = G(\xi,\eta) r \exp[i\varphi(\xi,\eta)](1-d(\xi,\eta)) + d(\xi,\eta) a_s \exp[i\varphi'(\xi,\eta)], \tag{5}$$

where $d(\xi, \eta)$ have random values uniformly distributed in the range [0, 1].

In our simulations, the intensity of the reference beam is chosen twice the average intensity of the object speckle beam and the effects of finite pixel size and the pixel quantization are neglected. Then, the average speckle size is defined as the ratio between the size of the fringe pattern and the radios ρ [9]. Computer simulations of speckle fringe patterns with different average speckle sizes are presented in Fig. 3.

3. DENOISING THROUGH THRESHOLDING IN TRANSFORM DOMAIN

Classical transform-based methods for additive noise removal are based on the assumption that most of the signal energy is compacted to a sparse set of significant transform coefficients while the noise is spread among all coefficients thus masking the insignificant ones. Their elimination should give a clean (denoised) signal estimate. The most correct way of performing the coefficient elimination is to use probabilistic models of both the information signal and the contaminating noise. If such models are too complex or not available, simplified models are adopted together with bounds limiting their use [16].

Consider a signal noise mixture, $z = y + r$, where y is the information signal, r is the contamination, assumed to be a zero-mean white noise of variance σ^2, i.e. $r \in \mathrm{N}(0,\sigma^2)$, and z is the observed signal. Without loss of generality, z, y, and r could be realizations of 1D or 2D processes measured on discrete grids, i.e. signals of length N or square images of size N^2. The decomposition of the mixture in a given orthonormal basis $\{\varphi_j\}_j^J$ is done through computing the inner products $\zeta_j = \langle z, \varphi_j \rangle$. Then, the transform coefficients are thresholded in a non-linear manner:

$$\hat{\zeta}_j = \begin{cases} \zeta_j, & if\left|\zeta_j\right| > \Gamma \\ 0, & \text{otherwise} \end{cases}, \tag{6}$$

and the denoised signal estimate is obtained from $\{\hat{\zeta}_j\}_1^J$ through the inverse transform. The non-linear threshold Γ is determined by the assumption of minimum risk. It has been shown that, for additive Gaussian noise model within image segment of size N^2, the so-called universal threshold can be used [13]:

$$\Gamma = \sigma\sqrt{2\ln N^2} \ . \tag{7}$$

The simple additive white Gaussian noise model is commonly assumed implicitly when denoising techniques are applied to experimental data. However, it does not fit to the complex form of noisy fringe patterns described by Eqs. (1-5). These equations suggest that a more realistic model for the noise in the fringe observation is a mixture of *multiplicative* noises, which essentially has a *signal-dependant* nature. Moreover, when the object deformation is large the noise also presents some decorrelation effects. Parameters of random processes involved in the fringe pattern formation are usually difficult to estimate during the measurements. Such parameters depend on the properties of the investigated object and from the experimental set-up. This makes the use of an accurate noise model quite difficult.

A local transform-domain processing would allow achieving a compromise between the ideal noise model and the commonly used additive white Gaussian noise model. While the noise is spatially varying on a global scale, we propose to model it as constant within the sliding window, assuming a local additive white Gaussian noise model. Thus, different thresholds shall be used for different part of the image depending on the local noise variance σ_n^2, where n is the index of the current local window. We favor DCT as a local transform. In contrary to wavelets, it is quite robust to speckles as fringe patters are captured in few coefficients of large amplitude, while speckles – being point singularities – are spread on a large number of low amplitude coefficients. This fact not only suggests that oscillatory transforms are better suited to fringe processing, but also hints that short-term correlation in the noise coming from the speckles is negligible, making the white noise assumption more realistic. As an oscillatory transform, Fourier transform would be also a suitable choice, however DCT is computationally less demanding. DCT is computed in a local window, sliding it one pixel at a time. Thus, a highly over-complete decomposition is obtained and multiple estimates of each pixel are obtained after thresholding and inverse transform. Their averaging allows compensating the Gibbs-like border distortions caused by the local processing [17].

The local noise variance can be estimated automatically in the DCT domain as the normalized median of the absolute value of the high-frequency coefficients:

$$\sigma_n = (0.6745)^{-1} \operatorname{median}_{j \in H} \left(\left| \left\langle z_n, \varphi_j \right\rangle \right| \right) \tag{8}$$

Here, z_n denotes the observed signal inside the local window, and H is a subset of high-frequency DCT coefficients containing, e.g. 50% of the high-end of the spectrum in a zig-zag scan.

While adopting the hard-thresholding scheme (6) in transform domain, we tune the universal threshold (7) by a user-adjustable parameter k in order to cope with the non-adequacy of the white Gaussian noise model:

$$\Gamma_n = k \sigma_n \sqrt{2 \ln N^2} \,. \tag{9}$$

For simplicity, the parameter k in (9) does not depend on the particular window n. Nevertheless, the resulting threshold Γ_n is locally adaptive as it depends on the local estimate of the noise variance. In the next section we present an analysis based on experiments that demonstrates the relationship between the optimal choice of k and the speckle size. Thanks to this analysis and to the local estimation of the noise, the transform-domain thresholding operation can be made fully automatic.

4. EXPERIMENTAL RESULTS

3.1. Experiments with simulated images

In order to compare with previous fringe pattern denoising methods, we adopt the following parameters the fidelity index f and the speckle index s:

$$f = 1 - \sum_{i,j=1}^{N} (I_{ij} - I_{ij\,original})^2 \Bigg/ \sum_{i,j=1}^{N} I_{ij\,original}^{2}\,, \qquad s = \frac{1}{N^2} \sum_{i,j=1}^{N} \frac{\sigma_{ij}}{\bar{I}_{ij}}\,, \tag{10}$$

where $I_{ij\,original}$ and I_{ij} are the intensities of the original and the nose image, σ_{ij} and $\bar{I}_{ij}$ are the local standard deviation and the local mean over a square 5x5 window respectively. The image fidelity measures how well image details are preserved after the filtering procedure. The speckle index s quantifies the local smoothness of the filtered fringe patterns. Its lower values indicate higher local smoothness. It can be regarded somehow as an average reciprocal of the signal to noise ratio.

In order to investigate and analyze the performance of the noise-suppression algorithms, we traced the behavior of the fidelity parameter f as a function of the tuning parameter k for different speckle sizes and window dimensions. The obtained results are presented graphically in Fig. 2. As it can be seen, the curve maxima for different speckle sizes follow almost identical behavior for different window dimensions. Subsequently, optimal tuning parameters k can be retrieved. So, in this study, we used k equal to 1.05, 0.94 and 1.10 for speckle sizes 1, 2, and 3 respectively.

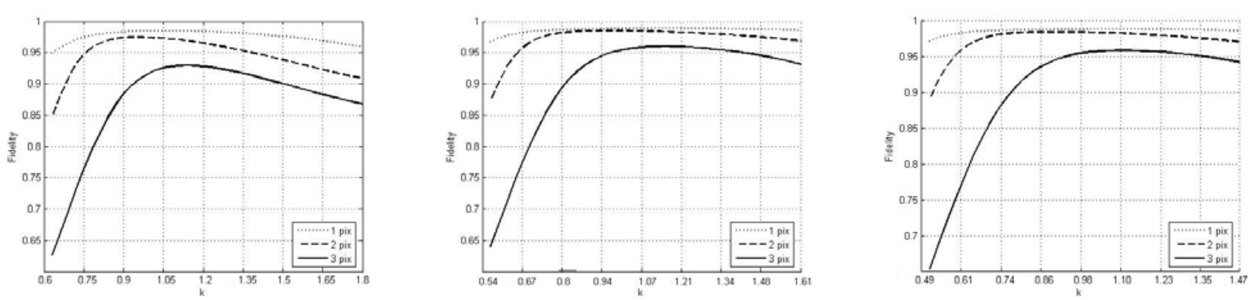

Fig. 2. The fidelity parameter f for different speckle and window sizes and for varying tuning parameter k.
From left to right: for windows of 16x16, 32x32, and 64x64 pix.

Fig. 3 visualizes results of the denoising procedure. The tuning parameter k has been chosen according the above comments. As seen, the denoised images are quite satisfying exhibiting clear speckle-free patterns.

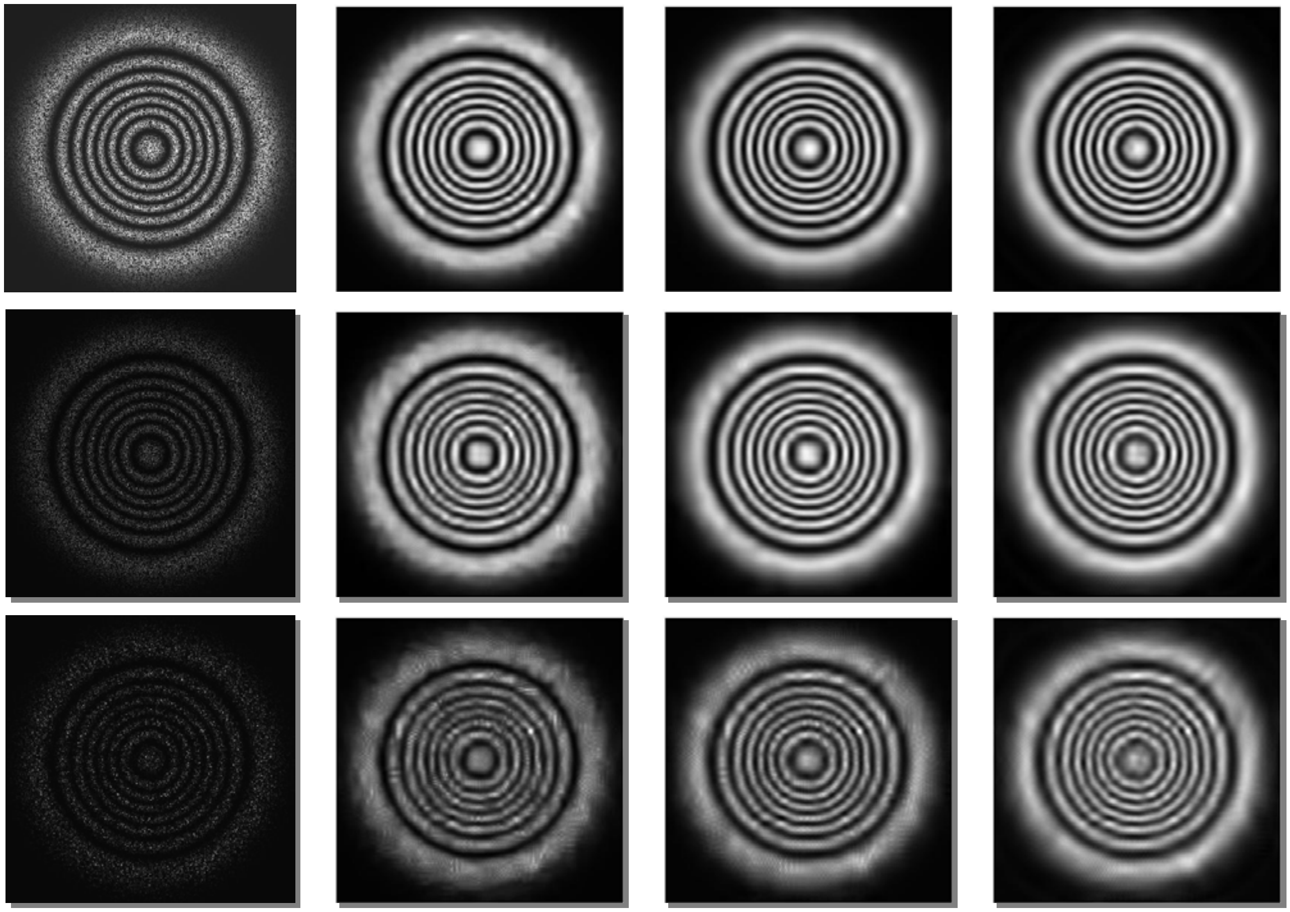

Fig. 3. Simulated speckle fringe patterns of size 384x384 pix. From top to bottom: average speckle size of 1, 2, and 3 pix. From left to right: noisy patterns, denoised with 16x16, 32x32, and 64x64 window sliding DCT.

In a next experiment, we take into account also the speckle pattern decorrelation effects, as described by Eq. (5). We compared our quantitative results with the methods from refs. [10], [12]. These results are summarized in Table 1.

The authors of [10] have applied wavelet transforms in a non-overlapping manner, i.e. as critically-sampled dyadic wavelet transform. Their thresholding scheme includes the universal threshold (i.e. assuming a global white Gaussian noise model) or even a linear low-pass filtering, which they call subband removal. While reproducing the wavelet experiments, we got worse results than those reported in [10]. This might be due to the slight difference in the experimental setting, and in order to be maximally fair we kept their best results. In any case our DCT-based technique performs considerably better due to the oscillating nature of the cosine basis functions, the local and over-complete processing and the properly tuned threshold.

Short-time Fourier transform, computed in a local, weighted and sliding manner is another choice of localizing transform. In the work [12], it is suggested that the Fourier-domain threshold should be controlled qualitatively (visually) and chosen in an 'interactive' manner. No assumptions about the noise model are made. While making simulations, we specified the window size and threshold as suggested in [12] and the results are given in the table. However, we believe that there is much better setting for this type of local Fourier-domain filtering. Such setting requires further research and we are working on it. A clear advantage of DCT vs. Fourier transform is that it is real-valued and therefore has been widely used in many image processing applications. Many specialized signal processors and integrated circuits performing fast DCT exist and can be used in real-time systems.

Table 1. Denoising results of different transform methods

Filter	Speckle Size	Fidelity f	Speckle Index s	Fidelity f	Speckle Index s	Filter	Fidelity f	Speckle Index s	Fidelity f	Speckle Index s
Decorrelation		Without		With			Without		With	
SDCT 16x16	1	0.985	0.20	0.947	0.13	Subband removal	0.92	0.14	Wavelet basis: Simmlet 8	
	2	0.974	0.18	0.918	0.12					
	3	0.916	0.16	0.825	0.10					
SDCT 32x32	1	0.988	0.19	0.969	0.13	Subband removal	0.92	0.13	Wavelet basis: Daubechies 10	
	2	0.984	0.20	0.954	0.13					
	3	0.931	0.16	0.886	0.10					
SDCT 64x64	1	0.989	0.19	0.970	0.13	Windowed Fourier 32x32	0.981	0.30	0.882	0.09
	2	0.985	0.19	0.954	0.12		0.960	0.26	0.838	0.12
	3	0.929	0.15	0.885	0.16		0.800	0.22	0.667	0.21

3.2. Experiment with real images

The proposed noise suppression approach has been applied to experimentally obtained speckle fringe patterns. The optical arrangement is a digital speckle-pattern interferometer with out-of-plane sensitivity. Two different objects have been investigated. The first one is a metal plate exposed to a thermal loading (Fig. 4). CCD camera with a matrix of 753x242 pix is used, and the average speckle size in this case is approximately 1.5 pix.

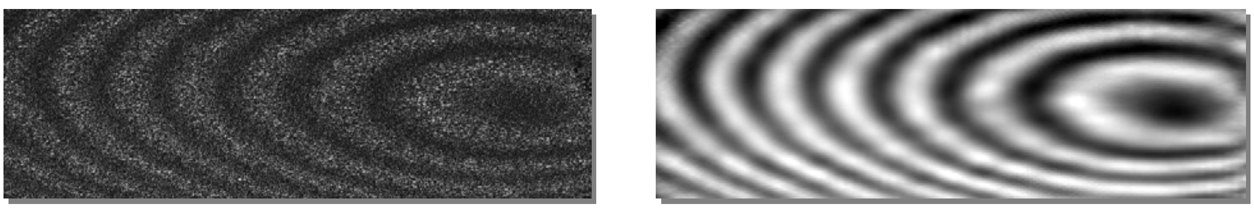

Fig. 4. Speckle fringe pattern obtained during thermal loading of a metal plate: the original and the filtered fringe pattern by means of an adaptive threshold SDCT filter with a window size 128x128 pix

The second object is a hollow cylindrical vessel made of fiber reinforced composite material. It is subjected to a high pressure loading which leads to its rapid deformations. The cylindrical shape of the object results in a nonuniform intensity distribution in the image plane. Another peculiarity of the experimental setup is the use of a speckled reference beam. This significantly simplifies the optical arrangement but also decreases the fringe pattern quality. The CCD camera matrix is with 1024x1024 pix and the frame capture rate is 30 fps. A fringe pattern acquired in the process of investigation is filtered and shown on Fig. 5.

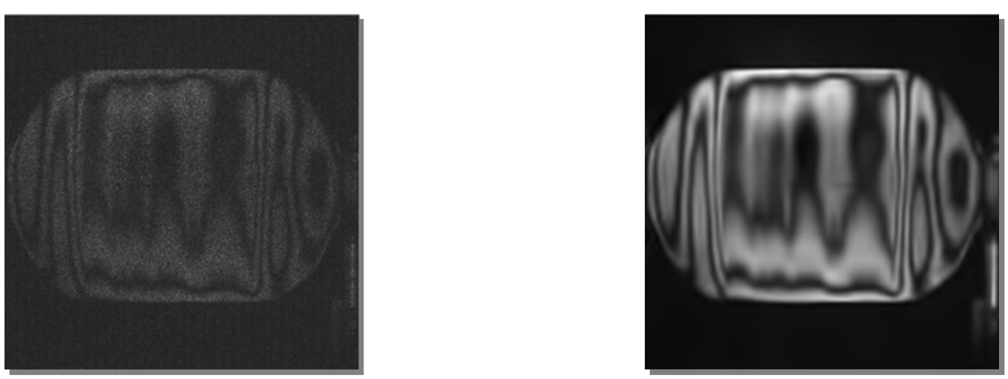

Fig. 5. Speckle fringe pattern obtained in the process of mechanical loading of a composite vessel: the original and the filtered fringe pattern by means of an adaptive threshold SDCT filter with a window size 128 x 128 pix

As could be seen, the denoised experimental fringe patterns are of high quality, the dense fringes are clearly distinguishable and not blurred. Such fringes can be further processed by means of simple tracing algorithms.

CONCLUSIONS

In this paper, we have studied a DCT-based denoising technique aimed at reducing speckle noise in DSPI fringe patterns. Properties such as over-completeness and local behavior were taken into account, discussed and properly utilized. These properties allow using a rather simplified noise model and an optimally-tuned threshold. Results obtained from simulated noisy patterns suggest an automated implementation of the technique. Denoising of real speckle fringe patterns have yielded nice-looking speckle-free images better suited for further processing (e.g. phase retrieval).

ACKNOWLEDGMENTS

The work of first three authors was supported by the EC within FP6 under Grant 511568 with the acronym 3DTV, while the fourth author was supported by grant No. 1521/05-TS, of the Bulgarian National Science Foundation.

REFERENCES

1. R. Jones, and C. Wykes, *Holographic and Speckle Interferometry*, Cambridge University, Cambridge, UK, 1983.
2. R. S. Sirohi (ed.), *Speckle metrology*, Marcel Dekker, New York, 1993.
3. P. K. Rastogi (ed.), *Optical Measurement Techniques and Applications,* Artech House Inc., Boston, London, 1997.
4. J. W. Goodman, *Statistical properties of laser speckle patterns*, in J. C. Dainty (ed.), *Laser Speckle and Related Phenomena*, Springer Series - Topics in Applied Physics, Vol. 9, Plenum Press, Berlin, 1975.
5. P. K. Rastogi, (ed.), *Digital Speckle Pattern Interferometry and Related Techniques*, John Wiley & Sons Ltd, Chichester, New York, 2001.
6. Th. R. Crimmins, *Geometric filter for speckle reduction*, Appl. Optics, **24**, No 16, 1438-1443 (1985).
7. Y. Qin, J. Chen, and H. Fan, *The study and application of a new filtering method on electronic speckle pattern interferometric fringe,* Optics and Lasers in Engineering, **39**, No. 4, 449-456 (2003).
8. H. Guo, J. E. Odegard, M. Lang, R. A. Gopinath, L W. Selesnick, and C. S. Burrus, *Speckle reduction via wavelet shrinkage with application to SAR based ATD/R*, in *Mathematical Imaging: Wavelet Applications in Signal and Image Processing*, Proc. SPIE, **2303**, 333-344 (1994).
9. G. H. Kaufmann, and G. E. Galizzi, *Speckle noise reduction in television holography fringes using wavelet thresholding*, Opt. Eng. **35**, No. 1, 9-14 (1996).
10. A. Federico, and G. Kaufmann, *Comparative study of wavelet thresholding methods for denoising electronic speckle pattern interferometry fringes*, Opt. Eng. **40**, No. 11, 2598-2604 (2001).
11. A. A. Shulev, I. R. Roussev, and V. Sainov, *New automatic FFT filtration method for phase maps and its application in speckle interferometry*, Proc. of SPIE, **4933**, 323-327 (2003).
12. Q. Kemao, *Windowed Fourier transform for fringe pattern analysis*, Appl. Optics, **43**, No. 13, 2695-2702 (2004).
13. D. Donoho, and I. Johnstone, *Ideal Spatial Adaptation via Wavelet Shrinkage*, Biometrica, **81**, 425-455 (1994).
14. T. Asakura, *Surface roughness measurements*, in Speckle Metrology, R. K. Erf (ed.), Academic Press, New York, pp. 11-49 (1978).
15. A. Federico, and G, Kaufman, *Local denoising of digital speckle pattern interferometry fringes by multiplicative correlation and weighted smoothing splines*, Appl. Optics, **44**, No. 14, 2728-2735 (2005).
16. S. Mallat, *A Wavelet Tour of Signal Processing*, Academic Press, 2002.
17. R. Öktem, L. Yaroslavsky, and K. Egiazarian, *Signal and image denoising in transform domain and wavelet shrinkage: a comparative study*, in Proc. of EUSIPCO'98, 9th European Signal Processing Conference, Rhodes, Greece, 8-11 September, pp. 2269-2272 (1998).

* assen@imbm.bas.bg; phone +359 2 9796403; fax +359 2 8707498